

# Numerical Simulation of Conveying Fine Powders in a Screw Conveyor Using the Discrete Element Method

Marko Motaln\*, Tone Lerher

**Abstract:** Due to their high efficiency and spatial utilization, screw conveyors are widely used in pharmacy, agriculture, and industry. Recently, this has made it a popular research subject in the numerical modelling of the transport of bulk solids. Modelling of granular systems at the level of individual particles is mainly possible due to the use of discrete numerical methods. The most common is the use of the Discrete Element Method (DEM), which is still limited from the point of view of simulations on an industrial scale, as increasing the size of the system also increases the cost of simulation. Certain powders with low density, large angles of repose, poor fluidity, and bad flowability can accumulate during transportation, causing inaccurate and non-uniform movement. Additionally, the friction and impact between the particles can cause wear. To address these issues, the present study utilizes the discrete element method to simulate and analyse powder transportation in an inclined screw conveyor using the commercial software ANSYS-ROCKY. Numerous phenomena that arise while transporting and feeding small-sized or irregularly shaped particles, often present in industrial processes, remain insufficiently investigated. This paper aims to analyse the transportation process of adhesive powders in a screw conveyor, with a focus on evaluating the impact of different screw blade speeds on transport. Multiple simulations were conducted, along with the implementation of an additional wear model, to better understand the transport phenomena and wear. An example was used to demonstrate the impact of screw speed on the wear of the transporter due to the interaction between the material and the structure of the conveyor, power consumption, and performance.

**Keywords:** abrasive wear; bulk handling; coarse graining; conveying equipment; discrete element method; screw conveyor

## 1 INTRODUCTION

In many industrial processes, it is crucial to maintain accurate control over the transportation of solid materials. Modern approaches to the numerical modelling of transport systems are based on advanced numerical methods. To adequately describe the transport of bulk materials and powders, it is necessary to understand and describe various phenomena that occur during the transportation of different bulk solids [1-3] in order to transport materials to the desired location, production plant, or machine. During transport, we deal with mixing, agglomeration of transported material, the flow behaviour of granular material, recirculation, wear, and many other phenomena that need to be utilized, suppressed, or applied for desired use [4-6].

One of the most commonly used methods for transportation of granular material and powder is the screw conveyor, which is widely utilized in the food, pharmaceutical, chemical, agricultural, and other industries due to its high efficiency, low cost, compact structure, and ability to provide uniform and precise feeding [7-9]. Screw conveyors are primarily utilized for transporting and lifting bulk materials and powders over short distances. The structure consists of an outer cylinder and an inner screw, but despite their seemingly simple mechanical design, the behaviour of granular solids and powders during transport is quite complex. Simulations of granular flow and describing phenomena that occurs during transport, such as wear, mixing, flow, pouring, or particle compaction, have already been included in the simulation in the past. It has been found that we can influence these phenomena with an appropriate design and construction of a transporter [3, 2]. There has been significant interest among the scientific community in studying the screw conveyor's conveying process. Therefore, substantial efforts have been made to describe the conveyors'

transportation parameters through conventional methods such as theoretical studies and experiments [7, 9]. Despite considerable efforts in academic research and traditional experimental techniques, a comprehensive understanding of the mechanisms underlying granular flows and their impact on the conveying performance of screw conveyors due to the lack of particle-level information remains unknown. Gaining deep insights into the system is challenging due to the difficulty in obtaining essential details such as particle collisions. With the rapid development of hardware, numerical simulation has emerged as an attractive tool for investigating and simulating complex particle systems. Modified geometry has been considered in many studies that have been conducted using spherical elements to approximate particles. If we highlight only a few, we can see that the first application of numerical modelling on a screw conveyor was already implemented back in 2001 by Shimizu and Cundall [10]. Since then, studies have been conducted on mixing granular media during transportation [11], granular flow, and performance with varying boundary conditions. Recently, we have witnessed a notable increase in the use of graphical processing units (GPU). The GPU-based algorithms in the discrete element method (DEM) have become increasingly popular for simulating complex and full-scale industrial processes, thanks to advancements in computer hardware. Several authors in their research have demonstrated the capabilities of multi-GPU computation and set benchmarks for successful simulations of large-scale industrial processes. These simulations accurately capture the behaviour of complex, non-spherical particles [12, 13]. As computer hardware, software, and numerical algorithms advance, we are gaining deeper insights into powder behaviour through complex geometries (e.g., polyhedral, elliptical elements, or multi-spheres). Cohesion and adhesion can influence the behaviour and flow of powder particles,

varying from one type of powder to another. Moreover, powders can often display characteristics of both liquids and solids, making them difficult to handle [14, 15]. The studies we have mentioned are based solely on spherical particles, which are not typically present in natural systems. A much more accurate approach is to capture the actual geometry of particles, which has been shown to have a significant impact on the granular flow of material [16]. Due to its exceptional importance and economic benefits, special attention has been given in the past to describing the wear during transport. Roughly a quarter of the world's energy consumption is derived from tribological contacts. Of this amount, around 20% is employed to conquer friction, while the remaining 3% is dedicated to the refurbishment of worn-out components and auxiliary equipment due to wear [17]. The economic impact of abrasive wear extends beyond replacement costs, encompassing expenses related to machine downtime and reduced productivity. Since the friction and wear caused by the movement of solid particles and powders during transportation can affect both the surface and the particles, accurate prediction of the location and magnitude of erosion in the equipment is essential to prevent the failure of devices. During the transportation of granules and powders, the primary types of wear mechanisms are impact wear and abrasion wear, which are also commonly observed in mining chutes [18]. Researchers have conducted many experimental and numerical studies to anticipate the wear of transport systems [19-21]. A new, exciting model called SIEM (Shear Impact Energy Model) has been recently proposed [22]. It is suitable for analysing sparsely or densely packed domains with particles in numerical simulations using the DEM method. It is based on the relationship between the normal and shear impact energy of a particle. The results show that almost one-fourth of the shear impact energy is converted into erosion and that the highest material removal rate is achieved at 30 degrees of impact. Furthermore, the lifespan of a chute heavily depends on the chosen material. Materials that exhibit higher resistance to abrasion wear, such as high chromium alloy and ceramics, are commonly chosen for this application [23-26]. Despite the numerous theoretical research and traditional experiments conducted in the past to optimize screw conveyor performance, they have their limitations in providing detailed particle-level information. This information is crucial in understanding the underlying mechanisms of granular and powder flows, which are essential in comprehending the phenomena and performance of screw conveyors. Additionally, powder flow is particularly poorly described in the literature, making it challenging to gain in-depth insights into the behaviour of powders. While simplified cohesion, complicated particle shape, and size distribution of particles are increasingly being considered, our understanding of these factors is still far from comprehensive. A study on screw auger is being conducted with the intention of evaluating powder flow in different screw auger speed regimes. A study is being conducted on screw auger to evaluate powder flow in different speed regimes. Coarse-graining techniques are being employed to analyse the effects of speed on power consumption, mass flow, and wear of the screw auger.

## 2 MATERIALS AND METHODS

Since the modelling approach is based on the Discrete Element Method (DEM), it is appropriate to provide a brief introduction to the DEM method in the following sections, as well as the corresponding models and modern approaches that were used in the numerical model.

### 2.1 Model Description

DEM is a widely used method for simulating the behaviour of granular flow. It is based on the Lagrangian description of individual particles, and the description of kinematics based on the principle of Newton's second law. The governing equations for individual particles can be expressed as follows:

$$m_i \vec{a}_i = m_i \frac{d}{dt} \vec{v}_i = \sum_{j=1}^{nc} \vec{F}_{ij} + \vec{F}_i^g + \vec{F}_i^{\text{ext}} \quad (1)$$

and

$$I_i \vec{\vartheta}_i = I_i \frac{d}{dt} \vec{\omega}_i = \sum_{j=1}^{nc} \vec{T}_{ij} + \vec{T}_i^{\text{ang}} + \vec{T}_i^{\text{ext}} \quad (2)$$

Since the method employs the Lagrangian numerical approach, each particle is represented as a separate entity with unique physical characteristics, including radius  $R_i$ , position  $\vec{x}_i$ , angle  $\vec{\varphi}_i$ , translational velocity  $\vec{v}_i$ , angular velocity  $\vec{\omega}_i$ , translational acceleration  $\vec{a}_i$ , and angular acceleration  $\vec{\vartheta}_i$ . The terms  $m_i$  and  $I_i$  are the mass and the inertia tensor of the particle  $i$ . The inertia term in the equation can be a scalar for spherical particles since they are symmetric, meaning the moment of inertia is equal in all directions. Due to the contacts with neighbouring particles, additional forces  $\vec{F}_{ij}$  and moments  $\vec{T}_{ij}$  arise in the particle, which is the sum of all neighbouring particle contacts. Due to the gravitational field and other external factors, there are also forces  $\vec{F}_i^g$ ,  $\vec{F}_i^{\text{ext}}$ , and moments  $\vec{T}_i^{\text{ang}}$ ,  $\vec{T}_i^{\text{ext}}$ , being a result of rolling friction between particles or other external moments between particles and geometry such as electrostatic, Van der Waals forces, or cohesive forces.

In the "soft sphere" approach model, we are dealing with rigid particles where deformation is simulated using overlap (superposition). We can introduce variables  $\delta_{ij}^n$  and  $\delta_{ij}^t$ , which denote normal and tangential overlap, respectively. An incremental approach is required to calculate the tangential overlap where  $\vec{v}_{\text{rel}}^t$  denotes relative velocity in the tangential direction.

$$\delta_{ij}^n = R_i + R_j - \|\vec{x}_j - \vec{x}_i\| \quad (3)$$

$$\delta_{ij}^t = \int_{t_0}^t \vec{v}_{\text{rel}}^t dt \quad (4)$$

Modelling a nonlinear viscoelastic model is currently one of the most widely used constitutive models in many software programs because it provides precise and efficient descriptions of contact loads for DEM analysis. This model incorporates nonlinear elasticity and enables the modelling of particle collisions in the tangential direction. Contact in

the normal direction is based on the work of physicist H. Hertz while the credit for describing tangential contact is attributed to the duo of Mindlin-Deresiewicz [27]. The used model is schematically represented in Fig. 1.

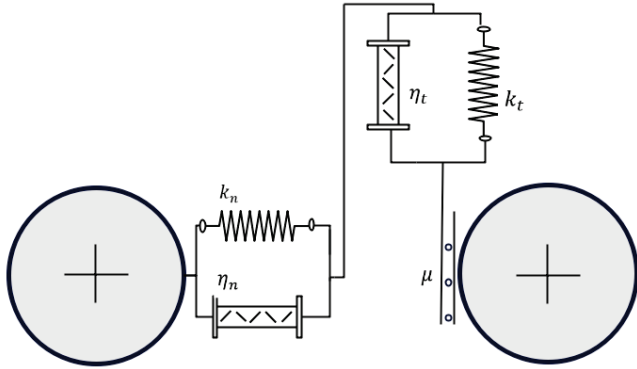


Figure 1 Hertz Mindlin contact scheme

The contact in the normal direction can be expressed as:

$$F_{ij}^n = k_n \delta^n \frac{3}{2} + \eta_n \delta^n \frac{1}{4} \vec{v}_{rel}^n \quad (5)$$

$$k_n = \frac{4}{3} E^* \sqrt{R^*} \quad (6)$$

$$\eta_n = 2 \eta_H \sqrt{k_n m^*} \quad (7)$$

Where  $E^*$ ,  $R^*$ , and  $m^*$  are effective Young's modulus, effective radius, and effective mass respectively. The stiffness coefficient  $k_n$  and damping coefficient  $\eta_n$  are represented in equations 5 and 6 [28]. Where  $\eta_H$  is described as the damping ratio and is for interested readers detailed described in [29].

Similar follows for contact in the tangential direction where the model in Rocky can describe friction coefficient  $\mu$  where its value is set to static coefficient  $\mu_s$  when no sliding occurs and similarly value is set to the value of dynamic coefficient  $\mu_d$  when sliding occurs. The resulting force can be described by the following equations [28]:

$$\vec{F}_{ij}^t = -\mu F_{ij}^n \left(1 - \zeta^2\right) \frac{\vec{\delta}^t}{|\vec{\delta}^t|} + \beta \sqrt{\frac{6 \mu m^* F_{ij}^n}{\delta_{MAX}^t}} \zeta^{\frac{1}{4}} \vec{v}_{rel}^t \quad (8)$$

$$\zeta = 1 - \frac{\min(|\vec{\delta}_{ij}^t|, \delta_{MAX}^t)}{\delta_{MAX}^t} \quad (9)$$

Where  $\beta$  is the tangential damping ratio and can be calculated from the coefficient of restitution as follows:

$$\beta = \frac{\ln(c_r)}{\sqrt{\ln^2(c_r) + \pi^2}} \quad (10)$$

The variables  $\vec{v}_{rel}^t$  and  $\delta_{MAX}^t$  are representing relative tangential velocity and maximal allowed tangential overlap, respectively. The reader can quickly determine that the variable  $\zeta$  in the equation becomes equal to 0 as soon as the tangential overlap exceeds the allowed limit. At that point,

the model becomes equivalent to the Coulomb model, and the force is equal to the product of  $\mu$  and  $F_{ij}^n$  [28].

The behaviour and flow of powder particles can be influenced by cohesion and adhesion. Several options are available for handling cohesive particles in DEM simulations. The most popular methods used in the overviewed literature [4, 30] are the van der Waals model and the JKR model. As a result of obtaining a material model (refer to section 2.4), which was calibrated using a simplified constant model, we have decided to adopt a similar model. This model applies a constant force  $\vec{F}_i^{adh}$  when separated normal overlap  $-s_n$  is smaller than prescribed adhesive distance  $\delta_{adh}$ . This model is the most basic one and can be expressed using the following equation [28]:

$$\vec{F}_i^{adh} = \begin{cases} 0 & \text{if } -s_n \geq \delta_{adh} \\ f_{adh} g \min(m_1, m_2) & \text{if } -s_n < \delta_{adh} \end{cases} \quad (11)$$

We obtained a system of three vector equations usually integrated in time using explicit time integration schemes. The most used procedures include the explicit Euler and velocity Verlet schemes because of their simplicity, stability, and low memory usage.

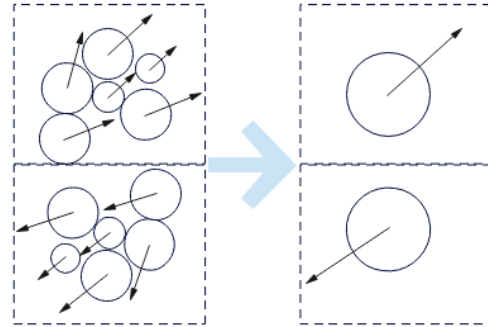


Figure 2 Coarse graining scheme

## 2.2 Coarse Graining

Despite significant advancements in accelerating discrete numerical simulations through GPU technology, precise simulations of real-world industrial systems are often unfeasible due to increasingly complex geometrical and physical models that address contact. This engineering challenge is particularly evident when using computationally expensive methods like the DEM, where obtaining sufficiently accurate results for a system at acceptable computational costs is a common problem. This involves introducing large pseudo-particles to represent a group of original particles, significantly reducing the number of particles needed for simulation [31]. The used method of particle merging is well presented in the article [32] and relies on correcting contact forces accordingly. The objective is to develop a medium that can scale particle sizes and maintain the same energy density and evolution of energy density as the basic model. If the density and volume fraction of the particle remains constant, the density of gravitational potential energy is not affected by the grain radius. Thus, it is necessary to maintain a constant density. In order to preserve kinetic energy, the scaling process must not

influence particle velocities. Similar studies have been conducted in articles [31, 33-36].

### 2.3 Wear Model

In DEM most frequently used are Archard or Finnie's model. Finnie developed a mathematical model based on mass, speed, and impact angle [18]. Archard's model, on the other hand, is based on the ratio between the shearing work and the overlapping volume and is also included in our simulation model [5]. Archard's phenomenological principle that correlates the loss of material volume to the energy expended by frictional forces acting on the material's surface. Typically, Archard's law is mathematically represented by the following equation [28]:

$$V = \frac{k W \tau}{H} \quad (12)$$

Where  $V$ ,  $W\tau$ ,  $H$ , and  $k$  respectively represent the total volume of material worn from the surface, the work done by tangential forces, the hardness of the material, and a dimensionless empirical constant. The fact that precise treatment of wear is a highly complex problem is confirmed by the dependence of wear on the size, shape, and chemical composition of particles. Increasing throughput performance and particle velocity typically result in higher wear rates. Based on the existing literature, it can be argued that the influence of particle characteristics such as shape, size (especially for powders), and adhesion on flow behaviours, conveying performance, and wear patterns in screw conveyors has not been thoroughly investigated. Consequently, this field presents several open challenges and research questions for future studies [16].

### 2.4 Simulation Model

The most reliable and verifiable models can be produced by calibrating materials using experimental results. Proper material calibration is essential, especially when there is insufficient computing power to solve full scale problems. For simulation previously described Coarse graining with ratio of 10 is employed, and calibration is required to produce the most reliable simulation data. For our numerical analysis, we extracted data from work [37], where full material calibration was performed with the inclusion of the coarse grain method and particle size distribution grouping.

**Table 1** Simulation parameters

| Value                         | Property                              |
|-------------------------------|---------------------------------------|
| $r = 0,000724$                | Particle radius (m)                   |
| $\rho_p = 712$                | Particle density (kg/m <sup>3</sup> ) |
| $\rho_g = 7850$               | Geometry density (kg/m <sup>3</sup> ) |
| $E_p = 18, E_g = 210$         | Young's modulus (GPa)                 |
| $\nu_p = 0,3, \nu_g = 0,3$    | Poisson ratio (-)                     |
| $\mu_p = 0,7, \mu_g = 0,35$   | Sliding friction (-)                  |
| $\mu_p = 0,7, \mu_g = 0,35$   | Rolling friction (-)                  |
| $c_{rp} = 0,83, c_{rg} = 0,8$ | Rest. Coefficient (-)                 |
| $n = 43000$                   | Particle count (-)                    |
| $d = 140$                     | Screw diameter (mm)                   |

Additionally, we repeated the calibration of the static angle of repose containing a rigid plane and lifting cylinder and used a constant adhesive model that is sufficient for most cases where the adhesive force is present which is true for most substances such as fine pharmaceutical powder or wet rocks. The parameters of the adhesive model were adjusted based on repeated calibration.

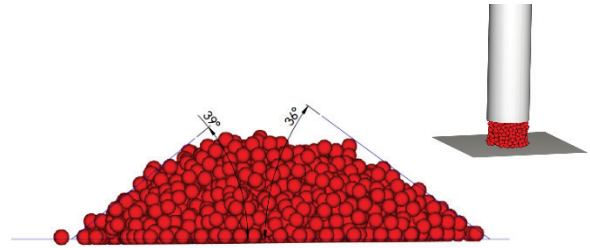


**Figure 3** Repetition of calibration with enlarged particles

A three-dimensional model of a typical powder steel screw conveyor has been modelled. A full geometry model can be shown on Fig. 4 and is assembled from a housing, screw, flanges, inlet, outlet chutes, and other standard elements like motor which are not shown. The inlet and outlet can typically be customized to meet the specific requirements of the work site. For the purposes of this simulation, a fixed inclination angle of 45° has been set. Properties or characteristics not visible in Fig. 4 can be found in Tab. 1.

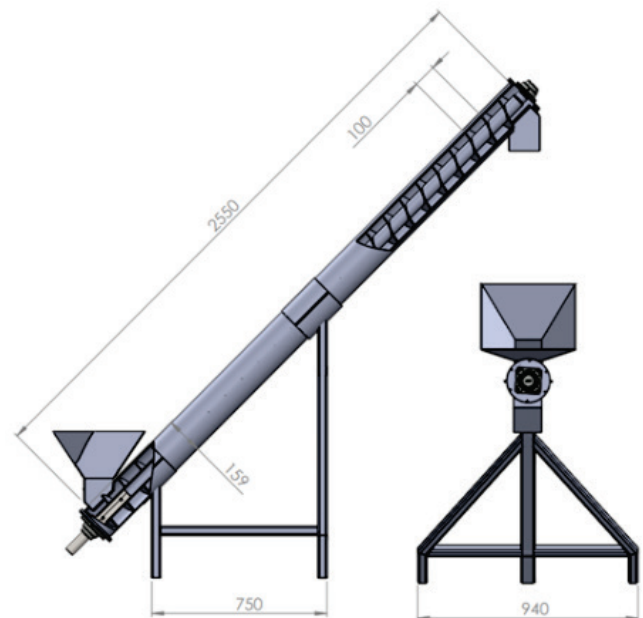


**Figure 4** Full inclined screw conveyor geometry

In addition to increasing the number of particles, an additional limitation was imposed for the purpose of numerical simulation due to limited computational power. To describe the behaviour of particles during transport, it was not necessary to model the entire transporter at full scale. Therefore, a simplified model was created which includes a feed port, a helical body, and a housing. To minimize computational power while ensuring that the flow resulting

from scattering or disposal sites has already stabilized in the observed area, the model was designed to reduce the length of the screw conveyor by an additional 2/3, while still maintaining an equivalent description of the original system.

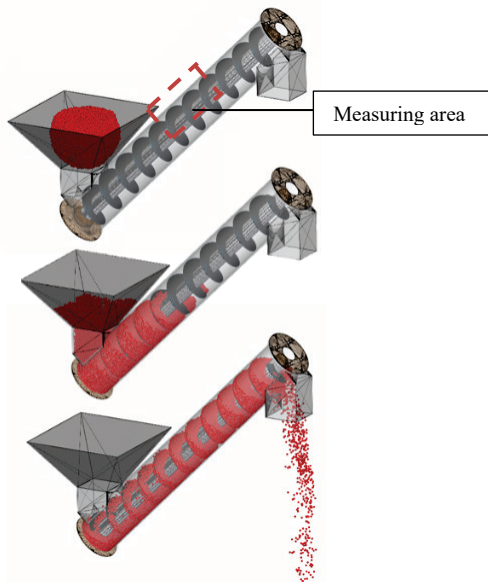


Figure 5 Simplified screw conveyor geometry

The simulation model for this research was created using Ansys-ROCKY 2022/R2. In a simplified model using a volumetric formula for particle creation at the point of the scattering site, an initial quantity of 4 kg of particles is generated. This quantity represents approximately 30% filling of the model container. This was followed by the activation of the screw rotation with variation of three rotational speeds (100 rpm, 300 rpm, and 500 rpm). Once the screw starts rotating, there is an initial transient state where the particles settle, and the stresses stabilize. The flow is allowed to stabilize before any measurements are taken. The simulation is repeated multiple times in different configurations of rotation speed and with or without an adhesion model. Simulation is continued until the container is emptied. Additional measuring points were created to provide a more detailed analysis of the geometric components and particles in different phases of the particle flow. Furthermore, measuring points based on Euler statistics were installed at the midpoint of the transporter tube (Fig. 5).

### 3 RESULTS AND DISCUSSION

The results are presented in two sections, with the first section focusing on mass flow and power consumption, and the second section describing the results of wear analysis.

#### 3.1 Mass Flow Rate

Fig. 6 shows the results of an analysis on the relationship between the rotational speed of the screw and the measuring area void fraction. The analysis reveals that increasing the rotational speed of the screw results in a higher void fraction. This is because particles have less time to fill the void in the

pitch of the screw at higher rotational speeds. Theoretically, the proportion of voids could be reduced by using an extended charging inlet in the hopper, but this is often not feasible in practice. Similarly, from Fig. 7, we can observe the void fraction as function of time. The peaks demonstrate a stable flow at maximum filling. Furthermore, as the rotational speed increases, we can observe a decrease in the height of the stable flow peak. This may be attributed to the decreasing weight of particles in the feed hopper over time. Therefore, the weight or amount of material in the hopper also affects the void fraction.

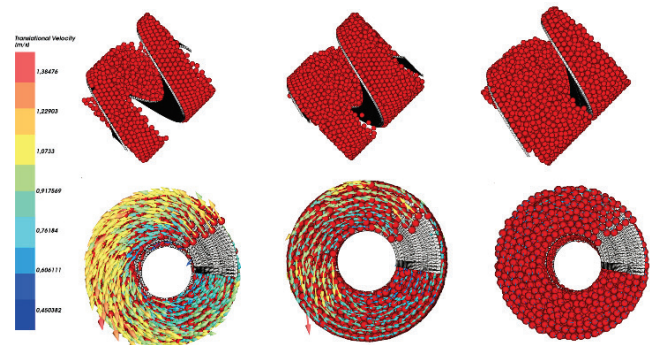


Figure 6 Flow of particles within a screw conveyor and the direction of particle flow when viewed along the axis of the conveyor.

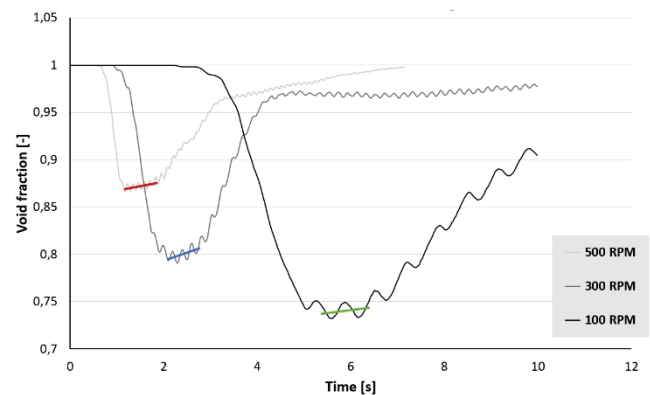


Figure 7 The void fraction of the control volume as a function of time

Despite the highest void fraction at the highest rotational speed, the results in Fig. 8 show that the mass flow rate of material is still the highest at the highest screw speed. The increase in mass flow rate seems to be nonlinear, as there is very little increase in mass flow rate between 300 and 500 revolutions per minute compared to the increase at lower angular speeds. The mass flow rate is calculated based on the calculation of the mass of particles that leave the control volume in a time step. The calculation must take into account the fact that some particles may return to the control volume due to the inclination of the conveyor.

The influence of cohesion can also be seen in a limited way in Fig. 8 which is denoted by the 'coh' sign on the graph. Similar to previous studies results show that cohesion have a significant effect on material flow. At the highest rotational speed, it is visible that the powder with cohesion has a lower mass flow rate, which is result of lower filling of the pitch. Since our material has relatively low adhesive force, these



phenomena are not particularly pronounced. It would be interesting to increase the adhesion and monitor the influence on porosity, filling, or other phenomena, such as arching.

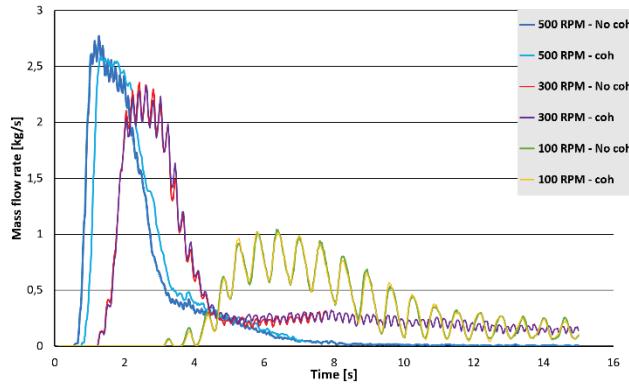


Figure 8 The Particle Mass flow rate in the control volume as a function of time

Through the application of DEM, one can conduct a thorough analysis of the way energy is distributed within a system. Specifically, the screw acts as a supplier of energy to the particles, whereby a certain proportion of this energy is dissipated, while the remaining portion is converted into mechanical energy. Fig. 9 demonstrates the power consumption of the screw auger at three different angular speeds. It can be clearly observed that the power consumption tends to increase with increasing screw rotation speed. The graph was analysed to calculate the ratio of power consumption to mass flow rate for all three angular velocities. Based on the limited data, it can be concluded that beyond a certain speed, the energy utilization changes less and tends to a constant value. This graph also provides insights into selecting the optimal angular velocity based on energy consumption.

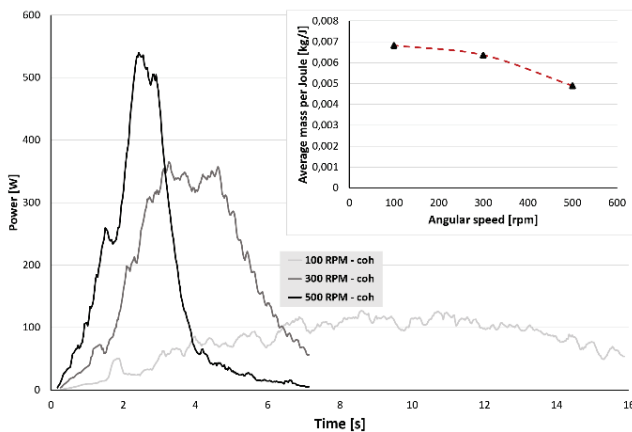


Figure 9 Power of the screw conveyor over time with an additional dependence of mass normalized to energy.

### 3.2 Wear Rate

Detailed information about the energy dissipated in each collision during the simulated period can be provided. Shear intensity refers to the amount of power that is transferred per unit area, and it is calculated based on the work done by the contact forces during a collision. This kind of energy is used

in abrasive wear models as the model is useful for determining shear wear on geometric surfaces. The model is applicable in determining shear wear on geometric surfaces and can be directly linked to wear. Fig. 10 illustrates a similar regime of increasing throughput performance and particle velocity, resulting in higher shear intensity of the screw over time.

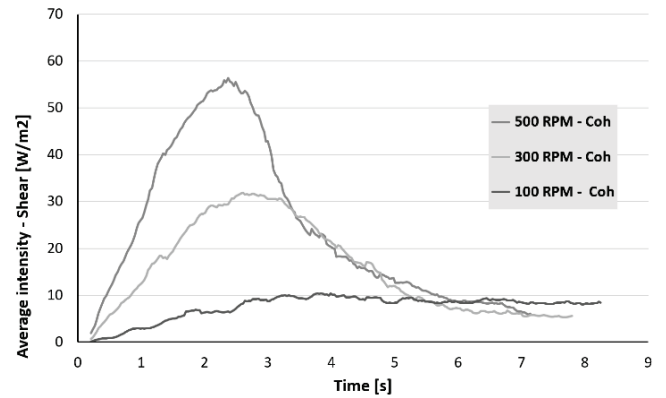


Figure 10 Shear intensity of the screw over time

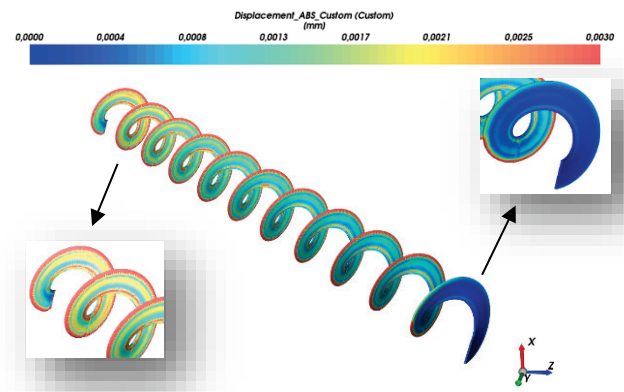


Figure 11 Screw wear rate distribution at 300 rpm

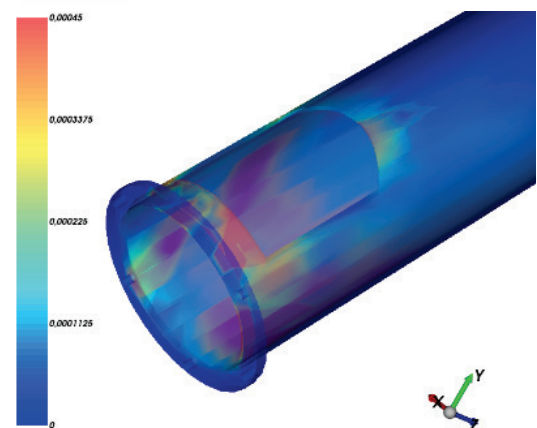


Figure 12 Housing wear rate distribution at 300 rpm

Wear was also described using the Archard wear model presented in section 2.4. It is particularly important to emphasize that in order to obtain an accurate quantitative description of wear, as shown in the images, it is necessary to determine the empirical wear constant correctly. As we did

not have access to this data within the scope of this study, the default value was used, and the description of wear is presented solely for the purpose of obtaining qualitative results, resulting in numerical results that may not be entirely accurate but are sufficient for an overview of the condition of the housing geometry, as the areas most exposed to damage. Wear can be presented in Figs. 11 and 12 for the screw and housing, respectively.

As shown in Fig. 11, the wear rate of the screw blade increases from the screw shaft toward the edge. The maximum wear occurs at the inlet where additional mass acting on the screw, results in greater wear over the entire surface. At the exit of the screw conveyor, only a few contacts are detected, resulting in minimal wear. Reverse side of the screw is due to its negligible amount of wear not considered.

#### 4 CONCLUSIONS

To gain a better understanding of transport phenomena and wear of adhesive powders in screw conveyor, multiple simulations were conducted, incorporating additional wear models. A brief overview of the literature used is presented, followed by a demonstration of the numerical modelling.

The void fraction and mass flow rate in the screw feeder were examined and expressed as a function of time. When varying the screw blade speeds, it was found that the void fraction in the screw conveyor increases as the speed increases. This phenomenon was attributed to the time constraints as particles are unable to sort in time at higher speeds. However, the mass flow rate increases with an increase in the screw blade speed. Limited results also demonstrate the impact of adhesion, resulting in lower mass flow rates. Power consumption of the screw auger was also evaluated for varying angular speeds, revealing that power consumption tends to increase as the screw rotation speed increases. The shear intensity and Archard wear model were used to demonstrate qualitative wear on the screw conveyor and housing. It was demonstrated that the system exhibits a tendency towards increased energy consumption and wear at higher particle speeds.

The study utilizes previously calibrated materials, which may limit the accuracy and reliability of the simulations. Further validation with real materials and simulation data is necessary to support the simulations. It would be worthwhile to explore the effects of increased adhesion on porosity, filling, and arching.

Reliable models require calibration using experimental results. With more precise input data and results, we can expect better solutions for the design of screw conveyors, reduced wear, and the selection of optimal rotational speeds. In the future, we aim to investigate the impact of particle wear without using coarse graining, using real particle shapes, which would require more accurate input data.

#### Acknowledgments

This research work was supported by the Slovenian Research Agency ARRS in the framework of the applied research project "Warehousing 4.0 – Integration model of

robotics and warehouse order-picking systems", grant number L5-2626.

#### 5 REFERENCES

- [1] Xia, R., Wang, X., Li, B., Wei, X., & Yang, Z. (2019). Discrete Element Method- (DEM-) Based Study on the Wear Mechanism and Wear Regularity in Scraper Conveyor Chutes. *Mathematical Problems in Engineering*, Article ID 4191570, 1-12. <https://doi.org/10.1155/2019/4191570>
- [2] Gelnar, D. & Zegzulka, J. (2019). *Discrete Element Method in the Design of Transport Systems: Verification and Validation of 3D Models*. Cham: Springer International Publishing. <https://doi.org/10.1007/978-3-030-05713-8>
- [3] Židek, M., et al. (2021). Effective use of DEM to design chain conveyor geometry. *Chemical Engineering Research and Design*, 167, 25-36. <https://doi.org/10.1016/j.cherd.2020.12.017>
- [4] Shi, Q. & Sakai, M. (2022). Recent progress on the discrete element method simulations for powder transport systems: A review. *Advanced Powder Technology*, 33(8), 103664. <https://doi.org/10.1016/j.apt.2022.103664>
- [5] Lee, S.-J., Lee, J.-H., & Hwang, S.-Y. (2022). Suggestion of Practical Application of Discrete Element Method for Long-Term Wear of Metallic Materials. *Applied Sciences*, 12(20), 10423. <https://doi.org/10.3390/app122010423>
- [6] Gelnar, D., Prokeš, R., Jezerska, L., & Zegzulka, J. (2021). Wood pellets transport with vibrating conveyor: experimental for DEM simulations analysis. *Scientific Reports*, 11(1), 16606. <https://doi.org/10.1038/s41598-021-96111-2>
- [7] Yu, Y. & Arnold, P. C. (1996). The influence of screw feeders on bin flow patterns. *Powder Technology*, 88(1), 81-87. [https://doi.org/10.1016/0032-5910\(96\)03107-5](https://doi.org/10.1016/0032-5910(96)03107-5)
- [8] Owen, P. J. & Cleary, P. W. (2009). Prediction of screw conveyor performance using the Discrete Element Method (DEM). *Powder Technology*, 193(3), 274-288. <https://doi.org/10.1016/j.powtec.2009.03.012>
- [9] Roberts, A. W. (1999). The influence of granular vortex motion on the volumetric performance of enclosed screw conveyors. *Powder Technology*, 104(1), 56-67. [https://doi.org/10.1016/S0032-5910\(99\)00039-X](https://doi.org/10.1016/S0032-5910(99)00039-X)
- [10] Shimizu, Y. & Cundall, P. A. (2001). Three-Dimensional DEM Simulations of Bulk Handling by Screw Conveyors. *J. Eng. Mech.*, 127(9), 864-872. [https://doi.org/10.1061/\(ASCE\)0733-9399\(2001\)127:9\(864\)](https://doi.org/10.1061/(ASCE)0733-9399(2001)127:9(864))
- [11] Pezo, L., Jovanović, A., Pezo, M., Čolović, R. & Lončar, B. (2015). Modified screw conveyor-mixers – Discrete element modeling approach. *Advanced Powder Technology*, 26(5), 1391-1399. <https://doi.org/10.1016/j.apt.2015.07.016>
- [12] Dong, Y., Yan, D., & Cui, L. (2022). An Efficient Parallel Framework for the Discrete Element Method Using GPU. *Applied Sciences*, 12(6), 3107. <https://doi.org/10.3390/app12063107>
- [13] Govender, N., Cleary, P. W., Wilke, D. N., & Khinast, J. (2021). The influence of faceted particle shapes on material dynamics in screw conveying. *Chemical Engineering Science*, 243, 116654. <https://doi.org/10.1016/j.ces.2021.116654>
- [14] Widartiningsih, P. M., et al. (2020). Coarse graining DEM simulations of a powder die-filling system. *Powder Technology*, 371, 83-95. <https://doi.org/10.1016/j.powtec.2020.05.063>
- [15] Thornton, C. & Yin, K. K. (1991). Impact of elastic spheres with and without adhesion. *Powder Technology*, 65(1-3), 153-166. [https://doi.org/10.1016/0032-5910\(91\)80178-L](https://doi.org/10.1016/0032-5910(91)80178-L)

- [16] Sun, H., Ma, H., & Zhao, Y. (2017). DEM investigation on conveying of non-spherical particles in a screw conveyor. *Particuology*, 65, 17-31. <https://doi.org/10.1016/j.partic.2021.06.009>
- [17] Holmberg, K. & Erdemir, A. (2017). Influence of tribology on global energy consumption, costs and emissions. *Friction*, 5, 263-284. <https://doi.org/10.1007/s40544-017-0183-5>
- [18] Ou, T. & Chen, W. (2022). On accurate prediction of transfer chute wear using a digital wear sensor and discrete element modelling. *Powder Technology*, 407, 117680. <https://doi.org/10.1016/j.powtec.2022.117680>
- [19] Chen, W., Biswas, S., Roberts, A., O'Shea, J., & Williams, K. (2017). Abrasion wear resistance of wall lining materials in bins and chutes during iron ore mining. *International Journal of Mineral Processing*, 167, 42-48. <https://doi.org/10.1016/j.minpro.2017.08.002>
- [20] Markov, D. P. (2022). Adhesion at friction and wear. *Friction*, 10, 1859-1878. <https://doi.org/10.1007/s40544-021-0564-7>
- [21] Archard, J. F. (1958). A crossed-cylinders friction machine. *Wear*, 2(1), 21-27. [https://doi.org/10.1016/0043-1648\(58\)90337-5](https://doi.org/10.1016/0043-1648(58)90337-5)
- [22] Zhao, Y., Ma, H., Xu, L., & Zheng, J. (2017). An erosion model for the discrete element method. *Particuology*, 34, 81-88. <https://doi.org/10.1016/j.partic.2016.12.005>
- [23] Yoganandh, J., Natarajan, S., & Babu, S. P. K. (2013). Erosive Wear Behavior of Nickel-Based High Alloy White Cast Iron Under Mining Conditions Using Orthogonal Array. *J. of Materi Eng and Perform*, 22(9), 2534-2541. <https://doi.org/10.1007/s11665-013-0539-6>
- [24] Wu, L., Guo, X., & Zhang, J. (2014). Abrasive Resistant Coatings—A Review. *Lubricants*, 2(2), 66-89. <https://doi.org/10.3390/lubricants2020066>
- [25] Xie, Y., Jiang, J. (Jimmy), & Islam, M. A. (2021). Applications of elastomers in slurry transport. *Wear*, 477, p. 203773. <https://doi.org/10.1016/j.wear.2021.203773>
- [26] Walker, C. I. & Robbie, P. (2013). Comparison of some laboratory wear tests and field wear in slurry pumps. *Wear*, 302(1-2), 1026-1034. <https://doi.org/10.1016/j.wear.2012.11.053>
- [27] Wang, Q. J. & Zhu, D. (2013). Hertz Theory: Contact of Spherical Surfaces. Wang, Q. J. & Chung, D. (Eds.). *Encyclopedia of Tribology*, Boston, MA: Springer US, 1654-1662. [https://doi.org/10.1007/978-0-387-92897-5\\_492](https://doi.org/10.1007/978-0-387-92897-5_492)
- [28] Rocky. (2022). ESSS Rocky, Release 2022 R2, DEM Technical Manual, ESSS Rocky DEM, S. R. L.
- [29] Antypov, D. & Elliott, J. A. (2011). On an analytical solution for the damped Hertzian spring. *EPL*, 94(5), p. 50004. <https://doi.org/10.1209/0295-5075/94/50004>
- [30] Sebastian Escotet-Espinoza, M., Foster, C. J., & Ierapetritou, M. (2018). Discrete Element Modeling (DEM) for mixing of cohesive solids in rotating cylinders. *Powder Technology*, 335, 124-136. <https://doi.org/10.1016/j.powtec.2018.05.024>
- [31] Mori, Y., Wu, C.-Y., & Sakai, M. (2019). Validation study on a scaling law model of the DEM in industrial gas-solid flows. *Powder Technology*, 343, 101-112. <https://doi.org/10.1016/j.powtec.2018.11.015>
- [32] Shimizu, Y. & Cundall, P. (2001). Three-Dimensional DEM Simulations of Bulk Handling by Screw Conveyors. *Journal of Engineering Mechanics*, 127(9). [https://doi.org/10.1061/\(ASCE\)0733-9399\(2001\)127:9\(864\)](https://doi.org/10.1061/(ASCE)0733-9399(2001)127:9(864))
- [33] Xu, L., Bao, S., & Zhao, Y. (2020). Multi-level DEM study on liner wear in tumbling mills for an engineering level approach. *Powder Technology*, 364, 332-342. <https://doi.org/10.1016/j.powtec.2020.02.004>
- [34] Cai, R. & Zhao, Y. (2020). An experimentally validated coarse-grain DEM study of monodisperse granular mixing. *Powder Technology*, 361, 99-111. <https://doi.org/10.1016/j.powtec.2019.10.023>
- [35] Radl, S., Radeke, C., Khinast, J. G., & Sundaresan, S. (2011). Parcel-Based Approach for the Simulation of Gas-Particle Flows.
- [36] Queteschiner, D., Lichtenegger, T., Pirker, S., & Schneiderbauer, S. (2018). Multi-level coarse-grain model of the DEM. *Powder Technology*, 338, 614-624. <https://doi.org/10.1016/j.powtec.2018.07.033>
- [37] Martinčević, N. (2017). Numerična analiza transporta sipkega materiala v procesu suhe granulacije. *MSc thesis*, Univerza v Mariboru, Fakulteta za strojništvo. (in Slovenian) <https://dk.um.si/IzpisGradiva.php?id=68896>

**Authors' contacts:**

**Marko Motaln**, MSc  
(Corresponding author)  
University of Maribor,  
(1) Faculty of Logistics,  
Mariborska cesta 7, 3000 Celje, Slovenia  
(2) Faculty of Mechanical Engineering,  
Smetanova ul. 17, 2000 Maribor, Slovenia  
marko.motaln2@um.si

**Tone Lerher**, Professor PhD  
University of Maribor,  
(1) Faculty of Logistics,  
Mariborska cesta 7, 3000 Celje, Slovenia  
(2) Faculty of Mechanical Engineering,  
Smetanova ul. 17, 2000 Maribor, Slovenia  
tone.lerher@um.si